

# Comparison of Olefin Copolymers as Compatibilizers for Polypropylene and High-Density Polyethylene

Yijian Lin,<sup>1</sup> Victoria Yakovleva,<sup>1</sup> Hongyu Chen,<sup>2</sup> Anne Hiltner,<sup>1</sup> Eric Baer<sup>1</sup>

<sup>1</sup>Department of Macromolecular Science and Engineering, Center for Applied Polymer Research, Case Western Reserve University, Cleveland, Ohio 44106-7202

<sup>2</sup>New Products–Materials Science, Core R&D, The Dow Chemical Company, Freeport, Texas 77541

Received 22 December 2008; accepted 3 February 2009

DOI 10.1002/app.30190

Published online 17 April 2009 in Wiley InterScience (www.interscience.wiley.com).

**ABSTRACT:** Some polyolefin elastomers were compared as compatibilizers for blends of polypropylene (PP) with 30 wt % high-density polyethylene (HDPE). The compatibilizers included a multiblock ethylene–octene copolymer (OBC), two statistical ethylene–octene copolymers (EO), two propylene–ethylene copolymers (P/E), and a styrenic block copolymer (SBC). Examination of the blend morphology by AFM showed that the compatibilizer was preferentially located at the interface between the PP matrix and the dispersed HDPE particles. The brittle-to-ductile (BD) transition was determined from the temperature dependence of the blend toughness, which was taken as the area under the

stress–strain curve. All the compatibilized blends had lower BD temperature than PP. However, the blend compatibilized with OBC had the best combination of low BD temperature and high toughness. Examination of the deformed blends by scanning electron microscopy revealed that in the best blends, the compatibilizer provided sufficient interfacial adhesion so that the HDPE domains were able to yield and draw along with the PP matrix. © 2009 Wiley Periodicals, Inc. *J Appl Polym Sci* 113: 1945–1952, 2009

**Key words:** compatibilizers; polyolefin elastomers; polypropylene/polyethylene blends

## INTRODUCTION

Polypropylene (PP) and high-density polyethylene (HDPE) are among the most abundantly used polymeric materials due to their mechanical robustness, low cost, and processability. The large amount of resulting waste of the two materials is of considerable concern. Recycling is one attractive way to deal with this problem. However, sorting the waste for recycling is a challenge in terms of cost and efficiency. An alternative approach is to blend the two materials without sorting them. Unfortunately, due to their incompatibility, the blends of PP and HDPE lose the ductility of the constituents and exhibit extremely low impact strength and tensile elongation.

Compatibilizers can reduce the interfacial tension and thus improve the interfacial adhesion between two blend constituents. Numerous studies have focused on the morphology and mechanical properties of PP/HDPE blends that were compatibilized with propylene–ethylene copolymer rubbers (EPR).<sup>1–5</sup> The ethylene segments were expected to be compatible with the HDPE phase and propylene segments were expected to be compatible with the PP phase. It was

found that in the compatibilized blends, the dispersed phase formed either a core-shell morphology with HDPE occlusions encased in rubber or an interpenetrated HDPE/EPR particle dispersed in the PP matrix, depending on the processing method.<sup>5</sup> The mechanical data showed that the modulus and yield stress were lowered upon the addition of EPR. However, the tensile elongation at break and the impact strength were significantly improved.<sup>2–5</sup>

Among the various chain structures, diblock or triblock copolymers are very attractive as compatibilizers. Theoretical results suggest that block copolymers form more interfacial bridges than statistical copolymers when the blocks are longer than the effective entanglement molecular weight.<sup>6,7</sup> Recently, The Dow Chemical Company developed a chain shuttling catalyst technology that can be used to synthesize novel olefin block copolymers (OBC) in a continuous process.<sup>8</sup> The block copolymers synthesized by chain shuttling technology consist of crystallizable ethylene/ $\alpha$ -olefin blocks with very low comonomer content and high melting temperature, alternating with amorphous ethylene/ $\alpha$ -olefin blocks with high comonomer content and low glass transition temperature. The new block copolymers have a statistical multiblock architecture with a distribution in block lengths and a distribution in the number of blocks per chain.

Correspondence to: A. Hiltner (ahiltner@case.edu).

Contract grant sponsors: The Dow Chemical Company.

It is believed that OBC will be a good compatibilizer for PP/HDPE blends. The low comonomer, crystalline blocks of an OBC should be compatible with the HDPE phase and the high comonomer, amorphous blocks should be compatible with the PP phase. A previous study showed that an OBC improved the interfacial interaction between PP and HDPE as evidenced by reduced HDPE domain size and increased elongation at break.<sup>9</sup> Stronger adhesion of the OBC to PP compared with a statistical copolymer was demonstrated by testing the delamination strength of one-dimensional model blends.<sup>10</sup> In the present study, OBC was compared with other polyolefin elastomers as a compatibilizer for PP/HDPE blends. The blend morphology was studied by atomic force microscopy (AFM). Correlations were sought between the tensile toughness and the deformation mechanisms as probed by scanning electronic microscopy (SEM).

## EXPERIMENTAL

Isotactic PP with density of  $0.900 \text{ g cm}^{-3}$  and HDPE with density of  $0.961 \text{ g cm}^{-3}$  were provided by The Dow Chemical Company (Freeport, TX). Copolymers used as compatibilizers for PP and HDPE blends were an ethylene–octene linear multi-block copolymer (OBC) (Dow Experimental OBC), two ethylene–octene statistical copolymers (EO855 and EO876), two propylene–ethylene statistical copolymers (P/E859 and P/E876), and a styrenic block copolymer (SBC) (Kraton<sup>®</sup> G1652) (Table I). The structure of the OBC was described previously.<sup>10</sup> The OBC had an overall octene content of 11 mol % and density of  $0.880 \text{ g cm}^{-3}$ . The OBC was 76% soft segment with octene content of 17 mol %. The hard segment of the OBC had 0.4 mol % octene. The EO855 had the same density and comonomer content (17 mol %) as the OBC soft segment. The EO876 had about the same density and overall comonomer content (11 mol %) as the OBC. The P/E859 had about the same density as EO855,  $0.859 \text{ g cm}^{-3}$  and  $0.855 \text{ g cm}^{-3}$ , respectively. The P/E876 had the same density as EO876 of  $0.876 \text{ g cm}^{-3}$ . The SBC was a styrene-(ethylene-butylene)-styrene block copolymer with density of  $0.910 \text{ g cm}^{-3}$ . The styrene/rubber ratio was 30/70.

Blends with composition PP : copolymer : HDPE (63 : 10 : 27 by wt) were prepared in a Haake (Karlsruhe, Germany) Rheomex TW-100 twin-screw extruder with average screw diameter of 25.4 mm and length-to-diameter ratio of 13/1. The barrel temperature was  $250^\circ\text{C}$  and the screw speed was 15 rpm. Uncompatibilized blends with composition PP : HDPE (70 : 30 by wt) were prepared with the same conditions.

The blends were pelletized and compression-molded at  $190^\circ\text{C}$  using a Carver (Wabash, IN) Model 3912 laboratory press. During compression molding,

**TABLE I**  
**Polymer Properties**

Polymer	MFI <sup>a</sup> ( $\text{g } 10 \text{ min}^{-1}$ )	Density ( $\text{g cm}^{-3}$ )	$T_g$ ( $^\circ\text{C}$ )	1% Secant modulus (MPa)
PP	3.2 <sup>b</sup>	0.900	18	–
HDPE	0.8 <sup>c</sup>	0.961	–	–
OBC		0.880	–42	$28 \pm 1$
SBC	5.0 <sup>b</sup>	0.910	–42 <sup>d</sup>	$26 \pm 1$
EO855	1.0 <sup>c</sup>	0.855	–39	$8 \pm 2$
EO876	3.0 <sup>c</sup>	0.876	–32	$15 \pm 1$
P/E859	2.0 <sup>e</sup>	0.859	–17	$15 \pm 1$
P/E876	2.0 <sup>e</sup>	0.876	–6	$160 \pm 20$

<sup>a</sup> Provided by the manufacturer.

<sup>b</sup>  $230^\circ\text{C}$ , 5 kg.

<sup>c</sup>  $190^\circ\text{C}$ , 2.16 kg.

<sup>d</sup> Soft phase of SBC.

<sup>e</sup>  $230^\circ\text{C}$ , 2.16 kg.

the blend pellets were sandwiched between two Mylar sheets, preheated at  $190^\circ\text{C}$  under minimal pressure for 8 min, compressed at 10 MPa for 5 min, and promptly quenched in another cold compression molder.

A small piece was cut from the sheets and microtomed at  $-85^\circ\text{C}$  through the thickness direction. The microtomed surface was examined with a Digital Instruments (Santa Barbara, CA) Nanoscope IIIa atomic force microscope (AFM).

Dog bone-shaped specimens were cut from the molded sheets for tensile testing according to ASTM D1708. The specimens had a thickness of 0.7 mm, a width of 4.8 mm, and a grip-to-grip separation length of 23.4 mm. An MTS (Eden Prairie, MN) Alliance RT/30 with an environmental chamber was employed to perform the uniaxial tensile tests at  $-40$ ,  $-20$ ,  $0$ ,  $21$ , and  $40^\circ\text{C}$  using a strain rate of  $100\% \text{ min}^{-1}$ . Additional tensile tests were performed at  $21^\circ\text{C}$  using strain rates of 10 and  $1000\% \text{ min}^{-1}$ .

Additional tensile specimens were stretched close to fracture at a strain rate of  $100\% \text{ min}^{-1}$  and  $21^\circ\text{C}$ . The blends compatibilized with OBC, EO855, P/E876, and SBC were stretched to a strain of 500%. The blend compatibilized with P/E859 was stretched to 425% and the uncompatibilized blend was stretched to 5%. A small piece was cut from stretched specimen and microtomed along the stretching direction at  $-85^\circ\text{C}$ . The microtomed surface was coated with  $150 \text{ \AA}$  of gold before it was examined in a JEOL (Tokyo, Japan) JSM 840-A scanning electron microscope (SEM).

## RESULTS AND DISCUSSION

### Blend morphology

The blend morphology was examined with AFM phase images. Some examples are presented in

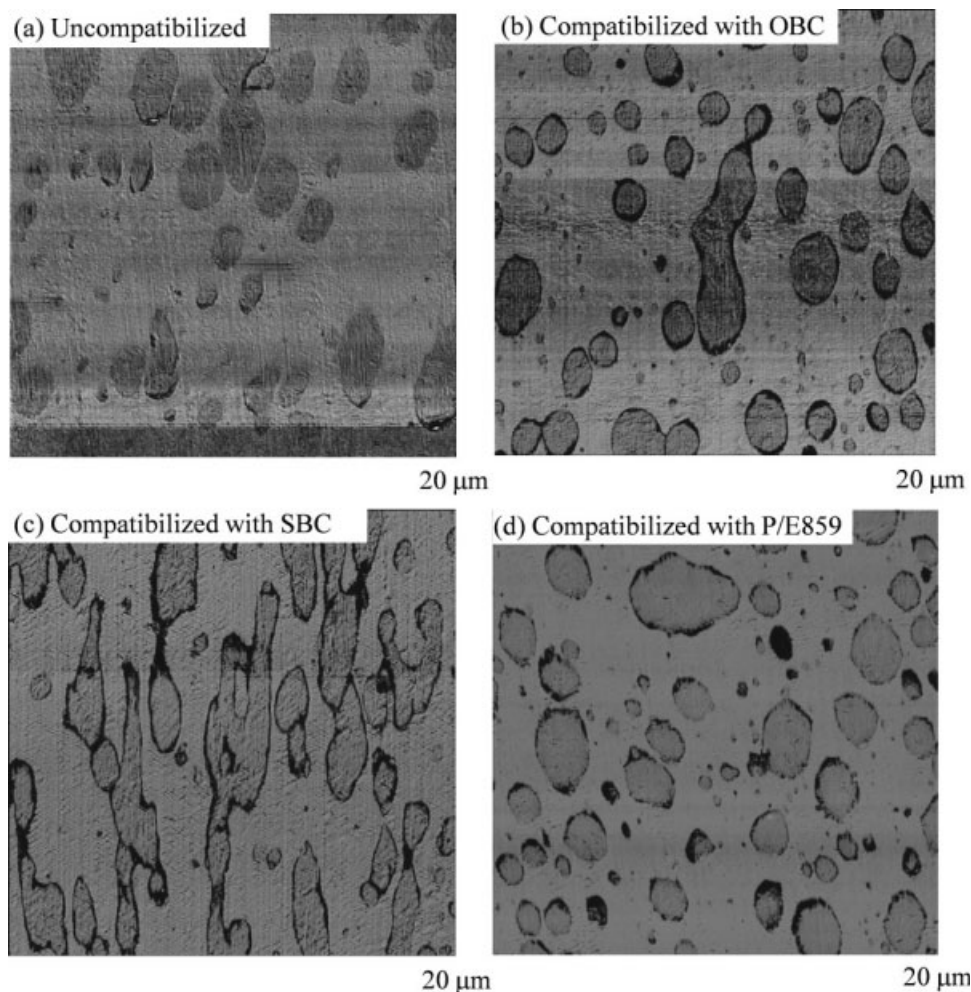


**Figure 1** Representative AFM phase images of PP/HDPE blends.

Figure 1. The amount of HDPE in the blends (30 wt %) was low enough that the HDPE phase was dispersed as domains in the PP matrix. In all cases, the domain size was about 1–4  $\mu\text{m}$ . A sharp interface was seen between the PP matrix and the HDPE particles in the PP/HDPE blends [Fig. 1(a)]. Occasional dark regions at the PP–HDPE interface were cracks that probably formed during the microtoming process. The fact that the cracks formed so easily suggests that interfacial adhesion was poor in the uncompatibilized blend.

In all the compatibilized blends, the dispersed HDPE particles were separated from the matrix by a thin, dark coating of the compatibilizer [Fig. 1(b–d)]. The compatibilizer appeared dark in the AFM images due to its low modulus. Although the copolymers did not reduce the HDPE domain size, it was apparent that they were preferentially located at the interface between PP and HDPE, where they could effectively reduce the interface tension and improve the interfacial adhesion.

### Tensile stress–strain behavior

The stress–strain curve of PP exhibited the typical necking, neck propagation, and strain-hardening behavior. Fracture occurred at a strain of almost 800% (Table II). The stress–strain curves for the PP/HDPE blends at a strain rate of  $100\% \text{ min}^{-1}$  and  $21^\circ\text{C}$  are shown in Figure 2. Without a compatibilizer, the PP/HDPE blend fractured at the yield point during neck formation. The fracture strain of PP/HDPE blend was less than 10% (Table II). The compatibilizers effectively improved the ductility of the PP/HDPE blends. All the compatibilized blends necked and yielded. Except for the blend compatibilized with EO876, which fractured during neck propagation at about 100% strain, all the compatibilized blends exhibited stable neck propagation with subsequent fracture in the work-hardening region. The highest fracture strains were observed for blends with SBC, OBC, and P/E876.

TABLE II  
Stress–Strain Results at 21°C

Material	1% Secant modulus (MPa)	Yield stress (MPa)	Yield strain (%)	Fracture stress (MPa)	Fracture strain (%)	Toughness (GPa)
PP	1560 ± 120	32 ± 1	8.9 ± 0.1	44 ± 1	770 ± 30	22 ± 1
HDPE	1020 ± 90	28 ± 1	7.0 ± 0.1	33 ± 1	940 ± 70	20 ± 2
PP/HDPE	1240 ± 10	30 ± 1	7.3 ± 0.1	30 ± 1	8 ± 1	0.2 ± 0.1
PP/(OBC)/HDPE	950 ± 30	23 ± 1	15 ± 2	32 ± 1	630 ± 20	14 ± 1
PP/(SBC)/HDPE	880 ± 10	23 ± 1	19 ± 1	38 ± 1	710 ± 10	18 ± 1
PP/(EO855)/HDPE	900 ± 20	20 ± 1	9.3 ± 6.0	23 ± 1	460 ± 20	8.8 ± 0.4
PP/(EO876)/HDPE	1000 ± 90	24 ± 1	9.0 ± 0.7	18 ± 1	120 ± 40	2.3 ± 0.7
PP/(P/E859)/HDPE	910 ± 10	20 ± 1	5.1 ± 0.4	20 ± 2	440 ± 40	7.7 ± 1.1
PP/(P/E876)/HDPE	1120 ± 30	25 ± 1	11 ± 2	30 ± 2	580 ± 60	13 ± 2

It is generally found that good stress transfer occurs at low strains, even in incompatible blends in the absence of a compatibilizer. Because HDPE is a thermoplastic that resembles PP in terms of mechanical properties, blending with HDPE did not substantially affect the low strain response. Consequently, the uncompatibilized PP/HDPE blend had modulus and yield stress close to those of PP. Compatibilization reduced the modulus and the yield stress significantly. The magnitude of the modulus reduction qualitatively correlated with the modulus of the compatibilizer (Tables I and II). A substantial modulus decrease was observed in other compatibilized blends including blends of polystyrene and linear low-density polyethylene compatibilized with various elastomeric block copolymers.<sup>11</sup> The modulus decrease was understood in terms of a core-shell particle that consisted of a compatibilizer shell surrounding the dispersed particle. Assuming that good adhesion existed between the phases, the effect of the rubbery shell was to lower the effective modulus of the particles by an amount that depended on

the modulus of the compatibilizer and the amount of compatibilizer in the shell.

The compatibilizer also affected the shape of the yield maximum in the stress–strain curve. Blends that were compatibilized with SBC, OBC, and EO855 showed a broader yielding region than the other blends. This probably resulted from the combined yielding of the PP and HDPE phases.

To compare the performance of the copolymers as compatibilizers for PP/HDPE blends, the toughness was calculated from the area under the stress–strain curve. The results showed that SBC, OBC, and P/E876 were the most effective, EO855 and P/E859 were intermediate, and EO876 was the least effective (Table II). Because the plateau stress and the strain-hardening slope were comparable in all the blends, differences in the toughness calculated by this method primarily reflected differences in the fracture strain.

#### Brittle-to-ductile transition

The brittle-to-ductile transition (BD) of polymer blends is an important performance characteristic

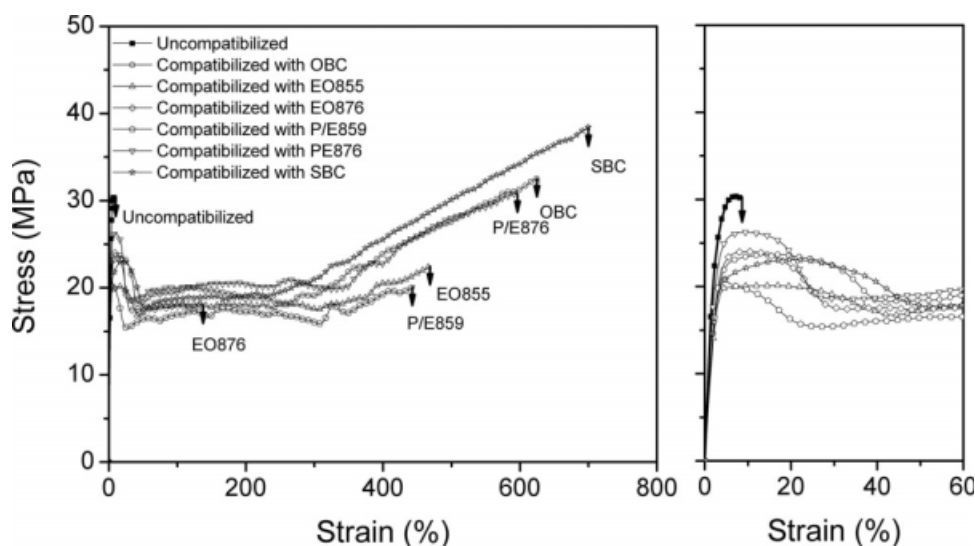
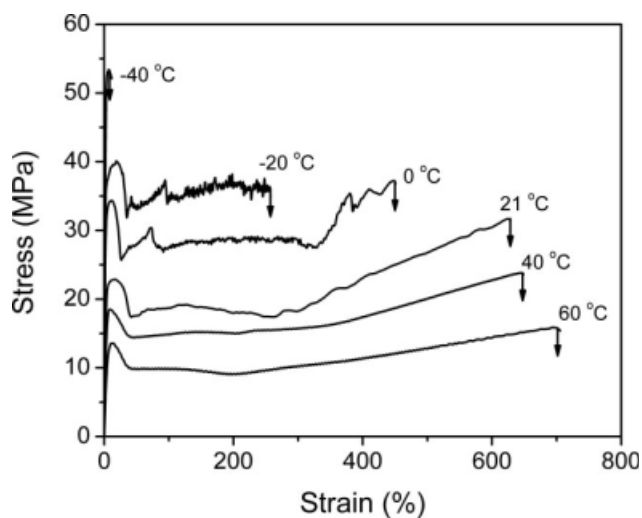


Figure 2 Stress–strain curves of PP/HDPE blends obtained at 21°C using a strain rate of 100% min<sup>-1</sup>. An expansion of the yield region is included.

that defines the use conditions. The BD of a ductile blend can be found by increasing the test rate or decreasing the test temperature. The BD of the PP/HDPE blends was initially sought by increasing the strain rate in the tensile test. However, tests at 100% and 1000%  $\text{min}^{-1}$  did not differentiate the compatibilized blends. The ductility at 100%  $\text{min}^{-1}$  was essentially the same as at 10%  $\text{min}^{-1}$ , and at 1000%  $\text{min}^{-1}$  all the blends fractured at low strain during neck formation and were classified as brittle.

The effect of temperature on the stress-strain behavior of PP/OBC/HDPE is shown in Figure 3. Not surprisingly, the modulus and yield stress increased, and fracture strain decreased, as the temperature was lowered. In this example, the BD occurred between  $-20$  and  $-40^\circ\text{C}$ , where the tensile response changed from stable neck propagation to fracture during neck formation.

Similar stress-strain measurements were made on all the blends, and the toughness was calculated from the area under the stress-strain curve (Fig. 4). The BD of PP occurred between 20 and  $0^\circ\text{C}$ , which coincided with the  $T_g$  of PP. All the compatibilizers lowered the BD to a temperature that correlated with the  $T_g$  of the compatibilizer. Thus, the BD of blends compatibilized with P/E copolymers occurred between 0 and  $-20^\circ\text{C}$  [Fig. 4(a)]. The BD of the blend with SBC as the compatibilizer was close to that of the P/E blends. The blends with OBC and EO copolymers had BD  $20^\circ$  lower, between  $-20$  and  $-40^\circ\text{C}$  [Fig. 4(b)]. It should be noted that the blend with EO876 exhibited poor toughness even above  $T_g$  in the ductile regime; nevertheless, a noticeable drop in toughness accompanied the  $T_g$ . A decrease in toughness of the blend with EO855 at higher temperatures was caused by gradual melting of the



**Figure 3** Effect of temperature on the stress-strain curve of the PP/HDPE blend compatibilized with OBC.

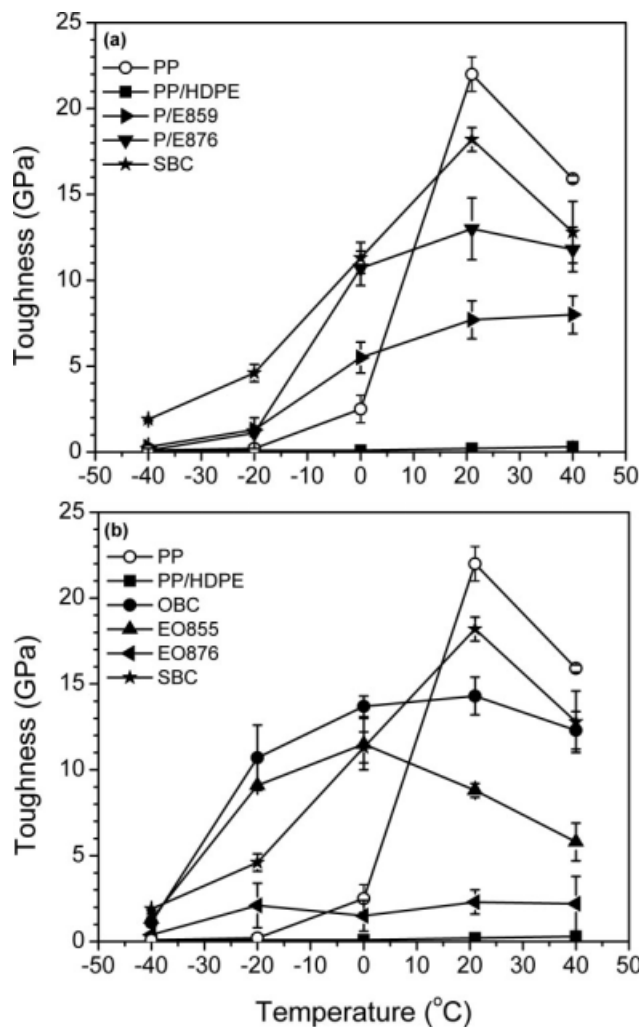


**Figure 4** Effect of temperature on the tensile toughness: (a) blends compatibilized with P/E copolymers and (b) blends compatibilized with ethylene-octene copolymers. Results for PP, the uncompatibilized blend, and the blend compatibilized with SBC are included.

crystalline phase between 0 and  $40^\circ\text{C}$ . Of the olefin copolymers, OBC was clearly the best compatibilizer having the highest toughness in the ductile regime and a low BD temperature.

#### Microstructure of stretched blends

The prefracture damage mechanisms were examined by SEM using specimens that had been stretched close to fracture. Typically, the necked region was examined; however, because the PP/HDPE control fractured at 8% strain without forming a stable neck, the image in Figure 5(a) shows a specimen that was deformed to 5% strain. The HDPE particles are undeformed, and large cracks are observed at the interface between PP and HDPE due to the poor interfacial adhesion. The specimen fractured when the cracks grew to critical size. All the

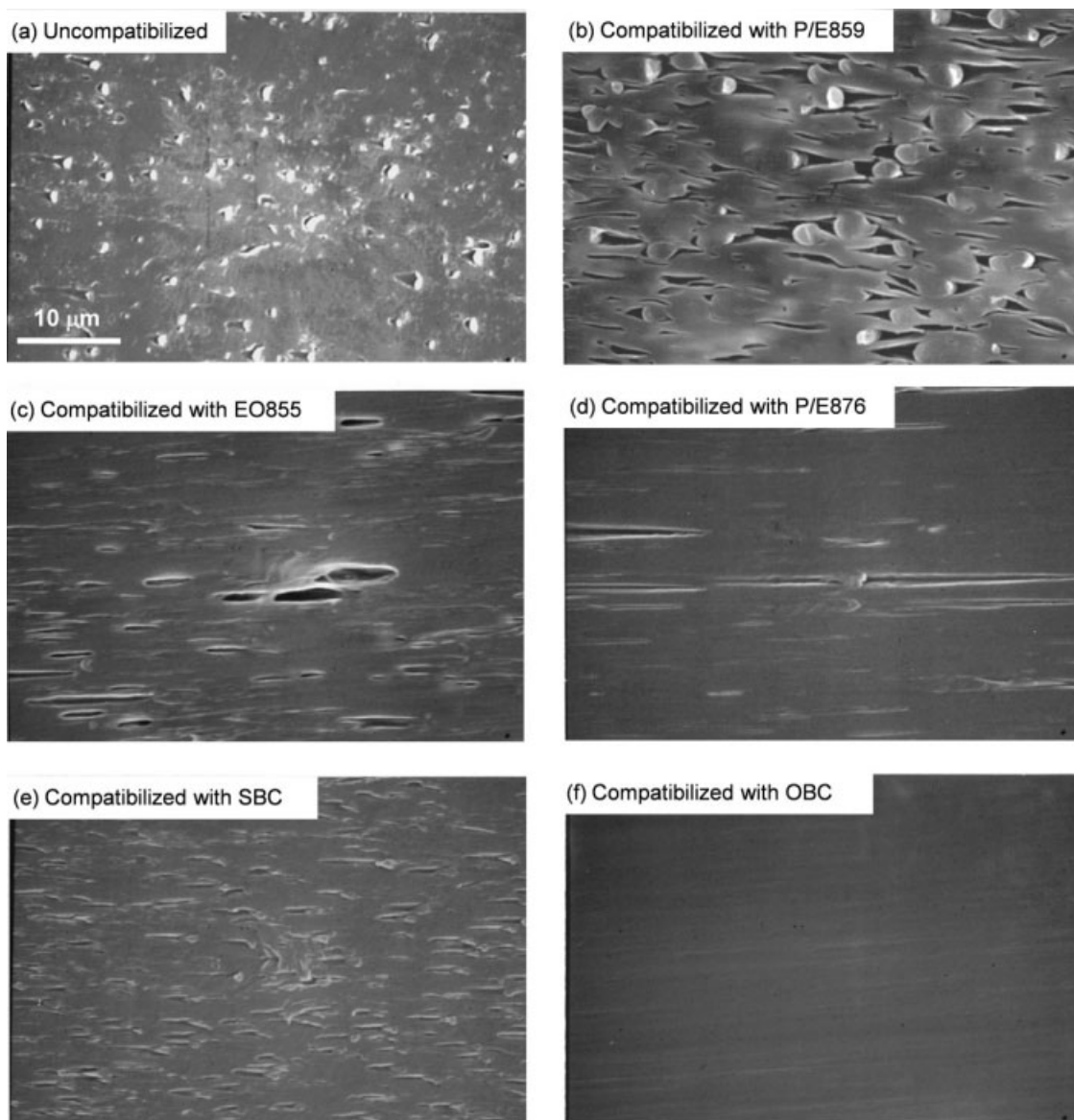


**Figure 5** SEM images showing the deformation mechanisms: (a) the uncompatibilized blend stretched to 5% strain; (b) the blend compatibilized with P/E859; (c) the blend compatibilized with EO855; (d) the blend compatibilized with P/E876; (e) the blend compatibilized with SBC; and (f) the blend compatibilized with OBC.

compatibilized blends except for the one compatibilized with EO876 exhibited stable neck propagation. The SEM images show specimens that were deformed to about 500% strain. The blend compatibilized with P/E859 shows numerous cracks that initiated at the poles of the HDPE particles [Fig. 5(b)]. Most of the HDPE particles retained their spherical shape after the matrix yielded. Apparently there was sufficient adhesion to prevent complete debonding and instead the cracks elongated as the PP matrix drew out around the particles. Nevertheless, this blend fractured at a lower strain than most of the other compatibilized blends. Undeformed HDPE particles were not seen in images of the blends com-

patibilized with EO855, EO876, OBC and SBC [Fig. 5(c–f)]. Rather, in these cases the adhesion was good enough that the particles were drawn out with the PP matrix. The combined yielding of PP and HDPE in blends compatibilized with SBC, OBC, and EO855 was already inferred from the broad yielding region in the stress–strain curve (Fig. 2). Cracks appeared to form where the interface failed at the tips of the drawn HDPE particles. The cracks were largest in the blend compatibilized with EO855 [Fig. 5(c)]. This blend also had a somewhat lower fracture strain. The cracks were smallest in the blend compatibilized with SBC [Fig. 5(e)], which was consistent with the higher fracture strain of this blend.

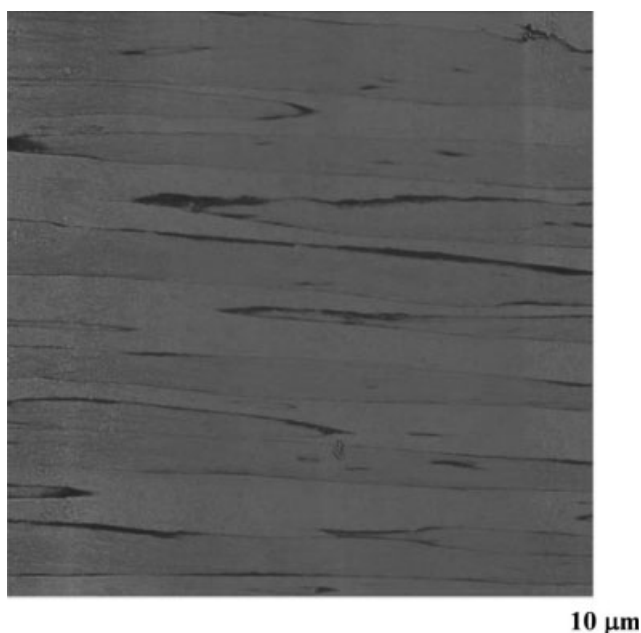


**Figure 6** AFM phase image of the blend compatibilized with OBC after stretching to 500%.

Only the blend compatibilized with OBC did not exhibit substantial cracking [Fig. 5(f)]. The SEM micrographs did not give a good contrast between the deformed HDPE particles and the PP matrix if there were no cracks at the interface. To confirm that the HDPE domains were stretched, the deformed specimen was examined with AFM. The HDPE appears as the darker, elongated domains in the phase image (Fig. 6). The HDPE and PP phases are separated by an irregular thin dark coating of OBC. In this case, adhesion was good enough that the interface did not fail, and instead good stress transfer between the particles and matrix enabled the HDPE particles to yield and draw along with the matrix.

In the elastic region, the interface was intact and the HDPE particles were load-bearing, even if the interfacial adhesion was poor. However, the high

local strains that accompanied matrix yielding increased the interfacial stresses dramatically. The particles started to debond and voids initiated at the poles where the tensile stress was highest. The extent of debonding depended on the strength of the interfacial adhesion.<sup>12,13</sup> The various failure modes that accompanied matrix yielding are shown schematically in Figure 7. If the adhesion was very poor, the HDPE particle detached from the matrix and the resulting void rapidly grew to the critical size for fracture initiation [Fig. 7(a)]. This was the case for the uncompatibilized PP/HDPE blend. If there was some level of adhesion, the HDPE particles did not completely detach from the PP matrix. Voids that formed at the poles of the HDPE particles lengthened in the loading direction [Fig. 7(b)] until the ligaments between voids broke and coalescence of the voids led to final fracture. The blend compatibilized with P/E859 provided an example of this failure mode. Because HDPE had a slightly lower yield stress than PP, the HDPE particles could yield and draw along with the matrix if the adhesion was good enough [Fig. 7(c)]. This was observed in blends compatibilized with EO855, EO 876, OBC, and SBC. Except for the blend compatibilized with OBC, small cracks appeared at the poles of the drawn particles; however, these appeared to survive to high strains before they were large enough to coalesce into critical size cracks.

## CONCLUSIONS

This study compared a number of polyolefin elastomers as compatibilizers for blends of PP and HDPE. Compatibilization with ethylene–octene or propylene–ethylene copolymers imparted almost the same toughness, as measured by the area under the ambient temperature stress–strain curve, as an SBC. These compatibilizers provided sufficient interfacial adhesion so that the HDPE domains were able to yield and draw along with the PP matrix. All the

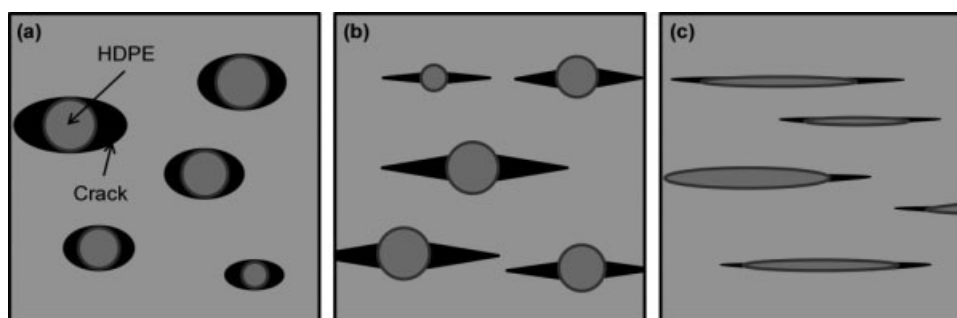


**Figure 7** Schematics showing the effect of adhesion on the deformation behavior: (a) poor adhesion; (b) somewhat better adhesion; and (c) good adhesion.

compatibilized blends lowered the BD of PP to a temperature that correlated with the  $T_g$  of the compatibilizer. However, due to the lower  $T_g$  of the ethylene–octene copolymers, the BD of blends compatibilized with these copolymers was about 20° lower than the BD of blends compatibilized with propylene–ethylene copolymers or SBC. In addition, a blocky ethylene–octene copolymer provided higher toughness than a statistical ethylene–octene copolymer.

The authors thank The Dow Chemical Company for their generous technical support.

### References

1. Teh, J. W.; Rudin, A.; Keung, J. C. *Adv Polym Technol* 1994, 13, 1.
2. Robertson, R. E.; Paul, D. R. *J Appl Polym Sci* 1973, 17, 2579.
3. Bartlett, D. W.; Barlow, J. W.; Paul, D. R. *J Appl Polym Sci* 1982, 27, 2351.
4. Nolley, E.; Barlow, J. W.; Paul, D. R. *Polym Eng Sci* 1980, 20, 364.
5. Stehling, F. C.; Huff, T.; Speed, C. S.; Wissler, G. *J Appl Polym Sci* 1981, 26, 2693.
6. Creton, C.; Kramer, E. J.; Hadziioannou, G. *Macromolecules* 1991, 24, 1846.
7. Creton, C.; Kramer, E. J.; Hui, C. Y.; Brown, H. R. *Macromolecules* 1992, 25, 3075.
8. Arriola, D. J.; Carnahan, E. M.; Hustad, P. D.; Kuhlman, R. L.; Wenzel, T. T. *Science* 2006, 312, 714.
9. Chen, H. Y.; Dias, P. S.; Poon, B. C.; Hiltner, A.; Baer, E. In *Proceedings of the Annual Technical Conference of the Society of Plastic Engineers*; SPE: Brookfield, Connecticut, 2007; Vol. 65, p 1201.
10. Dias, P.; Lin, Y. J.; Poon, B.; Chen, H. Y.; Hiltner, A.; Baer, E. *Polymer* 2008, 49, 2937.
11. Li, T.; Topolkaev, V. A.; Hiltner, A.; Baer, E.; Ji, X. Z.; Quirk, R. P. *J Polym Sci Part B: Polym Phys* 1995, 33, 667.
12. Li, T.; Topolkaev, V. A.; Hiltner, A.; Baer, E. In *Toughened Plastics II*; Riew, C. K.; Kinloch, A. J., Eds.; *Advances in Chemistry Series 252*; American Chemical Society: Washington, DC, 1996; p 319.
13. Li, T.; Carfagna, C.; Topolkaev, V. A.; Hiltner, A.; Baer, E.; Ji, X. Z.; Quirk, R. P. In *Toughened Plastics II*; Riew, C. K.; Kinloch, A. J., Eds.; *Advances in Chemistry Series 252*; American Chemical Society: Washington, DC, 1996; p 335.